

## ORIGINAL ARTICLE

# Targeted paclitaxel-octreotide conjugates inhibited the growth of paclitaxel-resistant human non-small cell lung cancer A549 cells in vitro

Yanguo Liu<sup>1</sup> | Handai Xia<sup>1</sup> | Yawei Wang<sup>1</sup> | Wenfei Han<sup>1</sup> | Jing Qin<sup>1</sup> |  
Wenjuan Gao<sup>2</sup> | Xun Qu<sup>2</sup> | Xiuwen Wang<sup>1</sup> 

<sup>1</sup>Department of Medical Oncology, Qilu Hospital, Cheeloo College of Medicine, Shandong University, Jinan, China

<sup>2</sup>Institute of Basic Medical Sciences, Qilu Hospital of Shandong University, Jinan, China

## Correspondence

Xiuwen Wang, Department of Medical Oncology, Qilu Hospital, Cheeloo College of Medicine, Shandong University, 107 Wenhuxi Road, Jinan, Shandong, 250012, China.  
Email: xiuwenwang12@sdu.edu.cn

## Funding information

Chinese Society of Clinical Oncology, Grant/Award Number: Y-QL2019-0376; National Natural Science Foundation of China, Grant/Award Number: 81874044; Natural Science Foundation of Shandong Province, Grant/Award Number: ZR2020MH236

## Abstract

The application of chemotherapy in non-small cell lung cancer (NSCLC) is limited by the toxicity to normal cells and the development of multi-drug resistance. Targeted chemotherapy using cytotoxic analogs against specific receptors on cancer cells could be a less toxic and more efficacious approach. We identified that the expressions of somatostatin receptor (SSTR) 2 and 5 in tumor tissues from NSCLC patients were higher than those in the adjacent normal tissues by immunohistochemistry, and therefore, cytotoxic somatostatin analogues might be applied for SSTRs-mediated targeted therapy against NSCLC. Two cytotoxic analogs, paclitaxel-octreotide (PTX-OCT) and 2paclitaxel-octreotide (2PTX-OCT), were synthesized by linking one or two molecules of paclitaxel to one molecule of somatostatin analog octreotide. PTX-OCT and 2PTX-OCT significantly inhibited the growth and induced apoptosis of SSTR2- and SSTR5-positive A549 cells, compared with the control ( $p < 0.01$ ), and had less inhibitory effect on SSTR2- and SSTR5-negative H157 cells than paclitaxel ( $p < 0.01$ ). Moreover, compared with paclitaxel, PTX-OCT conjugates induced lower expression of MDR-1 gene both in vitro and in vivo. Three A549 paclitaxel-resistant cell lines were established through different approaches, and the paclitaxel-resistant cell showed higher sensitivity to PTX-OCT conjugates than to paclitaxel, which might be because of the differential MDR-related gene expressions and cell-cycle distribution in paclitaxel-resistant A549 cells. Our results suggested that PTX-OCT conjugates could be potentially used for SSTRs-mediated targeted therapy for NSCLC, especially for those with paclitaxel resistance and induced less multidrug resistance.

## KEYWORDS

cytotoxic analogs, non-small cell lung cancer, paclitaxel resistance, somatostatin receptors

## INTRODUCTION

Lung cancer is still the leading cause of cancer-related deaths both in men and women in the world<sup>1</sup> as well as in China.<sup>2</sup> There are two major types of lung cancer, non-small cell lung cancer (NSCLC) and small cell lung cancer (SCLC), the former of which accounts for ~85% of all lung cancer cases.<sup>3</sup> Despite the advances in surveillance and early detection, NSCLC is often diagnosed at an advanced stage and has a poor prognosis.

Chemotherapy is one of the main treatments for advanced NSCLC patients, and paclitaxel (PTX) is used as first-line regimen in combination with cisplatin or as radio-sensitizing agents with therapeutic radiation. Unfortunately, although PTX shows positive effect on many NSCLC patients, its efficacy is often limited by the development of drug resistance. Chemo-resistance can be intrinsic or acquired; intrinsic resistance is pre-existent or inherent, whereas acquired resistance is induced by drug exposure.<sup>4</sup> There are a variety of mechanisms for PTX resistance, including altered expression and mutation

of  $\beta$ -tubulin, changes of apoptotic regulatory proteins, over-expression of cytokines such as interleukin 6 (IL-6) or ATP-binding cassette (ABC) that induces multidrug resistance (MDR).<sup>5</sup>

Targeted chemotherapy is a modern approach in cancer treatment, which aims to improve the therapy efficacy and decrease the peripheral toxicity.<sup>6,7</sup> Peptide receptors on malignant tumors can be used as targets by linking peptide ligands to cytotoxic agents, and several targeted cytotoxic analogues have already been developed and applied in the treatment of various types of cancer.<sup>8</sup> Somatostatin receptors (SSTRs) are a group of G-protein-coupled receptors that have been characterized in different types of cancer, including NSCLC.<sup>9</sup> SSTRs are found to be overexpressed in human NSCLC by radio-labeled analogues of somatostatin<sup>10,11</sup> and therefore, it could serve as potential targets for treatment. Cytotoxic somatostatin analogues containing doxorubicin or 2-pyrrolino-doxorubicin have been evaluated for treatment of colorectal cancer,<sup>12</sup> breast cancer,<sup>13</sup> glioblastoma,<sup>14</sup> etc.

Our group incorporated PTX into paclitaxel-octreotide (PTX-OCT) or 2paclitaxel-octreotide (2PTX-OCT) conjugates by linking one or two molecules of PTX to one molecule of somatostatin analog octreotide. We found that the cytotoxic conjugates inhibited the growth of human NSCLC cells both in vitro and in nude mice.<sup>15,16</sup> In this study, we established three A549 PTX-resistant cell lines through different approaches, evaluated the cytotoxic effect of targeted analogues on PTX-resistant sublines, and investigated its possible mechanisms. Acquired resistance can be induced by PTX through multiple mechanisms, including MDR.<sup>17,18</sup> MDR can be induced by increased exporting chemotherapeutic agents from cancer cells because of overexpressed ABC transporters, such as MDR-1, MDR-related protein 1 (MRP-1), and breast cancer resistance protein (BCRP).<sup>19</sup> The effect of targeted conjugates on the induced expressions of MDR-1, MRP-1, and BCRP was also investigated in this study both in vitro and in vivo.

## MATERIALS AND METHODS

### Case selection

A total of 118 previously untreated patients, who had undergone radical surgery or biopsy in Qilu Hospital, Shandong University and were diagnosed as NSCLC by pathology reports from 2017 to 2018, were reviewed. The subjects included 86 male and 32 female with a median age of 59 years old (range: 29–79). Adjacent lung tissues (>2 cm from original tumor margins) from 15 patients (10 male and 5 female; age range: 35–72 years old) were analyzed as control. The clinic-pathologic information of all cases, including age, sex, smoking history, histological type, primary tumor size, nodal status, and metastases, was collected. The study was approved by the Institutional Review Board of Qilu Hospital of Shandong University.

## Immunohistochemistry

Paraffin-embedded tumor samples were sectioned at a thickness of 4  $\mu$ m and placed on clean slides for immunohistochemical analysis. Polyclonal antibodies against SSTR2 (diluted 1:100; Boster) or SSTR5 (diluted 1:2000; Abcam) were added onto the slides after blocking with goat sera. Immunostaining was performed using SP kit and DAB kit (Zhongshan Goldenbridge Biotechnology) according to the manufacturer's instructions. Negative control was processed with phosphate-buffered saline (PBS) solution instead of primary antibodies. Slides were observed under an inverted microscope (Olympus IX81) and photographed with a digital camera.

## Peptide and cytotoxic conjugates

Octreotide was synthesized by Zillion Pharmaceutical (Shanghai, China), and the two conjugates, PTX-OCT and 2PTX-OCT, were synthesized and purified as previously described.<sup>15,16</sup>

## Cell culture and establishment of PTX-resistant cell lines

Human NSCLC cell lines H157 and A549, as well as A549 PTX-resistant derivatives, A549-P, A549-PS, and A549-S, were maintained in RPMI 1640 medium (Hyclone) containing 10% fetal bovine serum (Gibco) at 37°C in a humidified atmosphere with 5% CO<sub>2</sub>. A549 cells were selected for PTX resistance by different approaches as following.

### High dose pulse exposure (A549-P)

A549 cells were exposed to 3000 nM PTX (Shunyuan Chemtech) for 1 h, and then the medium was replaced. After achieving normal growth, the cells were exposed to 3000 nM PTX for 1 h, and the pulse exposures were repeated for a total of 10 times.

### Low dose stepwise exposure (A549-S)

A549 cells were initially exposed to 2.5 nM PTX. Once normal growth was achieved, the cells were maintained at the current concentration of PTX before gradually increasing it to 5 nM and 10 nM.

### Low dose stepwise exposure following high dose pulse exposure (A549-PS)

A549 cells were exposed to 3000 nM PTX for 1 h, and then maintained in medium with 2.5 nM PTX. After achieving

normal growth, the concentration of PTX was increased to 5 nM and 10 nM.

## Cell proliferation assay

H157, A549, and three A549 PTX-resistant cells were seeded into 96-well plates at a density of 1000 cells/well, respectively. After culturing for 24 h in the humidified incubator at 37°C and 5% CO<sub>2</sub>, PTX or cytotoxic conjugates of final gradient concentrations from 1 nM to 10 μM were added to each well. After 96 h, cell viability was assessed by 3-(4,5-dimethylthiazol-2-yl)-2,5-diphenyl tetrazolium bromide (MTT) assay. Briefly, 20 μL MTT (5 mg/mL in PBS, Sigma-Aldrich, USA) was added to each well and incubated for 4 h, then the medium was discarded and replaced with 150 μL dimethyl sulfoxide (DMSO, Sigma-Aldrich). The plates were shaken for 10 min for mixing and the absorbance was read at 570 nm by using a microplate reader with a reference filter of 630 nm (Bio-Rad). Cell viability was expressed as percentages, with that of the control setting as 100%. The drug concentration that reduced the viability of cells by 50% (IC<sub>50</sub>) was determined by cell inhibition rate, and the drug resistance index (RI) was equal to the ratio of IC<sub>50</sub> for resistant cell line to that for A549 cells.

## Cell apoptosis assay

Approximately  $2 \times 10^5$  A549 or H157 cells were plated into 6-well plates for 24 h. Cell apoptosis was induced by 10 nM PTX or PTX-OCT conjugates. After 48 h of induction, the cells were harvested, washed with cold PBS, and then re-suspended in  $1 \times$  binding buffer (BD Pharmingen). Approximately  $1 \times 10^5$  cells in 100 μL buffer were stained with 5 μL FITC-conjugated Annexin V (BD Pharmingen) and 5 μL propidium iodide (PI) (BD Pharmingen, USA) at room temperature for 15 min in the dark. After staining, 400 μL of  $1 \times$  binding buffer was added for analyzing by flow cytometry (BD FACScan, USA) within 30 min.

## Cell-cycle analysis

Approximately  $1 \times 10^6$  A549 or the PTX-resistant cells were collected, re-suspended, and fixed in 70% ethanol at -20°C overnight. The cells were stained with 0.5 mL PI/RNase staining buffer (BD Pharmingen, USA) for 15 min at room temperature and analyzed by flow cytometry (BD FACScan, USA). Histograms generated by fluorescence-activated cell sorting (FACS) were analyzed by ModFit software (BD, USA) to determine the percentage of cells in each phase (G1, S, and G2/M).

## In vivo experiment

Four-to-six-week male athymic nude mice (Ncr *nu/nu*) were obtained from Shanghai SLAC Laboratory Animal Co. (Shanghai, China). The mice were housed in laminar air-flow cabinets under special pathogen-free conditions, and fed with autoclaved standard chow and water at 26°C to 28°C with 40% to 60% humidity. All animal experiment protocols were reviewed and approved by the Ethics Committee of Shandong University.

Approximately  $5 \times 10^6$  A549 cells were injected into the right flanks of 20 male nude mice by subcutaneously. When tumors had grown to an average of 60 mm<sup>3</sup> in volume, the mice were randomly assigned into four groups: group 1 (control, 5 mice) received vehicle solution; group 2 (5 mice) was injected with PTX; group 3 (5 mice) was injected with PTX-OCT; group 4 (5 mice) was given 2PTX-OCT. The injections were conducted through tail vein on Days 1, 7, and 21 at a dosage of 150 nmol/kg. On Day 42, the mice were euthanized under anesthesia, followed by excising tumors and measuring the weight. Approximately 100 mg of the tumor tissue from each sample was used to isolate RNA according to the TRIzol reagent protocol (BBI).

## RNA extraction and synthesis of cDNA

Total RNA was isolated using TRIzol reagent (BBI and purified with RNeasy mini spin columns (Qiagen, USA). Then, 1 μg of the total RNA was subjected to reverse transcription into cDNA using TaKaRa RNA PCR Kit (Takara Bio) according to the manufacturer's protocol.

## Detection of mRNA for SSTRs by RT-PCR

PCR amplification was performed using target-specific primers to detect the mRNA expression of SSTR as previously described.<sup>15</sup> *β-actin* was co-amplified as an internal control.

## Real-time qPCR analysis of MDR-1, MRP-1, and BCRP

The gene-specific PCR primers were designed for MDR-1, MRP-1, and BCRP as previously reported.<sup>20</sup> qPCR was performed based on the LightCycler system (Roche Diagnostics). All the procedures were conducted according to the manufacturer's experimental protocol. The relative expression of each gene was calculated with Lightcycler software as the concentration of each target gene divided by the concentration of housekeeping gene *β-actin*. Melting curve analysis confirmed the specificity of the amplification products for the target genes.

## Statistical analysis

The values were reported as mean  $\pm$  standard deviation (SD), and significance was assessed by Student's *t* test or one-way ANOVA. Differences with  $p < 0.05$  were considered statistically significant.

## RESULTS

### Immuno-histochemical analysis of SSTR2 and SSTR5 expressions in tumor samples from NSCLC patients

We examined the expressions of SSTR2 and SSTR5 in 118 NSCLC samples by immunohistochemistry using specific antibodies. SSTR2 expression was mainly observed in membrane (Figure 1a, adenocarcinoma; Figure 1c, squamous cell carcinoma) whereas SSTR5 was expressed in both membrane and cytoplasm (Figure 1b, adenocarcinoma; Figure 1d, squamous cell carcinoma). The presence of SSTR2 and SSTR5 was 63% (74/118) and 61% (72/118) in the tumor samples, respectively; whereas the presence was significantly ( $p < 0.05$ ) lower in adjacent normal lung tissues, as 13% (2/15) (SSTR2, Figure 1e) and 20% (3/15) (SSTR5, Figure 1f), respectively.

### Expression of SSTRs in A549 and H157 cells

The mRNA of all SSTRs, except for SSTR4, was detected in A549 cells, and the mRNA expression of SSTR2 was relatively high (Figure 2a). SSTR2, SSTR3, or SSTR5 was not expressed in human H157 NSCLC cells, and only weak expressions of SSTR1 and SSTR4 were detected in H157 cells (Figure 2b).

### SSTRs-mediated cytotoxicity of PTX-OCT conjugates

PTX-OCT and 2PTX-OCT had similar inhibitory effects on SSTR2-, SSTR3-, and SSTR5-negative H157 cells, whereas their toxicity (0.1 nM to 10  $\mu$ M) on H157 cells was significantly ( $p < 0.01$ ) lower than that of PTX (Figure 3a). We have previously shown that PTX-OCT and 2PTX-OCT inhibited the growth of A549 cells in time- and dose-dependent manners (0.1 nM to 10  $\mu$ M at 24, 48, and 72 h).<sup>15</sup> In this study, we treated SSTRs-positive A549 cells for 96 h, and found that A549 cells were less sensitive to PTX-OCT than to PTX, which was reflected by the significantly ( $p < 0.01$ ) higher IC<sub>50</sub> for PTX-OCT (221.35  $\pm$  10.60 nM) than for PTX (65.35  $\pm$  7.94 nM), whereas no significant difference in IC<sub>50</sub> values was found between 2PTX-OCT and PTX (Table 1).

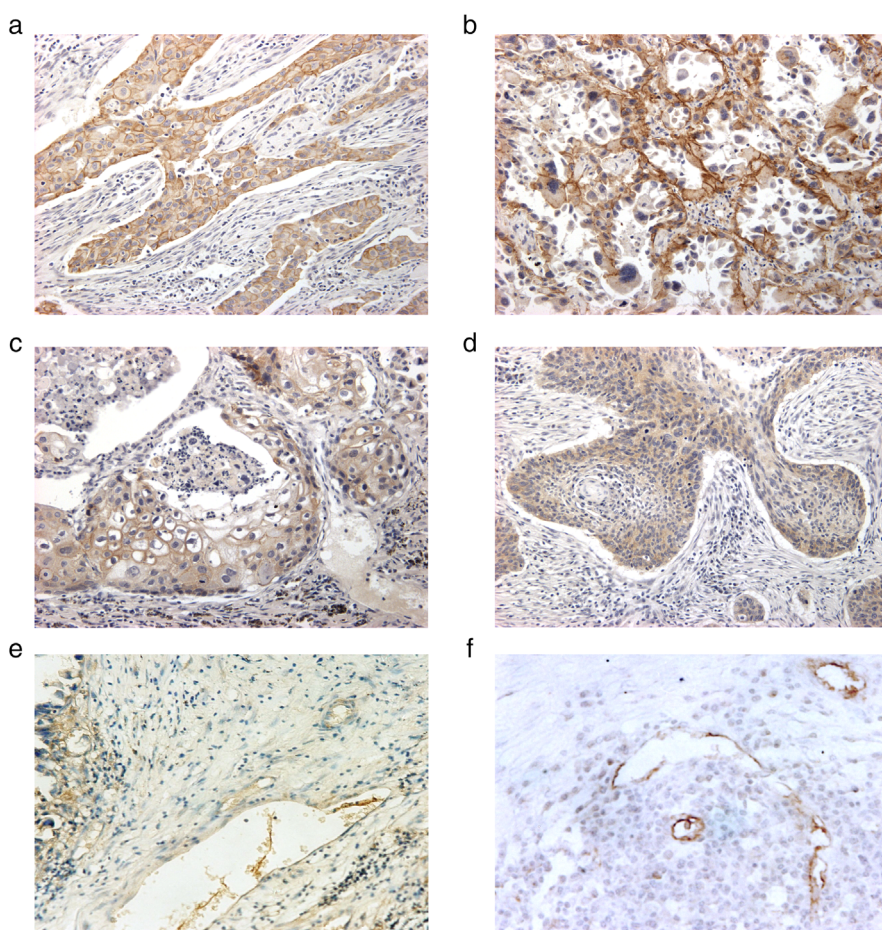


**FIGURE 1** Expression of somatostatin receptor (SSTR) 2 and 5 in specimens from non-small cell lung cancer (NSCLC) patients. Immuno-histochemical analyses were performed to detect the distribution of SSTR2 and SSTR5 in NSCLC specimens. Strong diffuse membrane expression of SSTR2 was observed in both lung adenocarcinoma (a) and squamous cell carcinoma (c) ( $\times 200$ ); SSTR5 with both cytoplasmic and membranous distribution was also detected in adenocarcinoma (b) and squamous cell carcinoma (d) of lung ( $\times 200$ ). In the adjacent lung tissues, the expressions of SSTR2 (e) and SSTR5 (f) were weaker ( $\times 200$ ) and with lower frequency in the positive cases

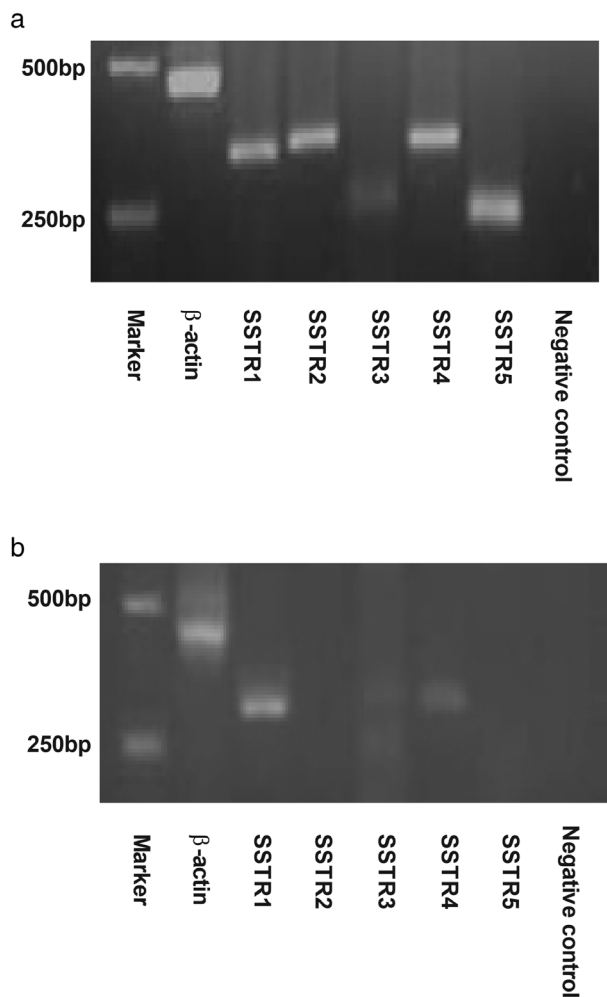


**FIGURE 2** The mRNA expressions of somatostatin receptor (SSTR) subtypes 1–5 in A549 and H157 cells. In A549 cells, the mRNA expressions of all SSTRs except SSTR3 (a) were detected, whereas only SSTR1 and SSTR4 mRNA expressions were detected in H157 cells (b)

It is well documented that PTX can induce apoptosis in cancer cells including NSCLC cells.<sup>21</sup> Apoptosis assay revealed that 10 nM PTX could induce apoptosis in an average

of 15.72% A549 cells ( $p < 0.01$  versus control). PTX-OCT and 2PTX-OCT also induced apoptosis in A549 cells ( $p < 0.01$  versus control), whereas the effect by PTX-OCT was significantly ( $p < 0.05$ ) less than that by PTX (Figure 3b). Although apoptosis of H157 cells was also induced by PTX-OCT or 2PTX-OCT treatment ( $p < 0.05$ , PTX-OCT versus control;  $p < 0.01$ , 2PTX-OCT versus control), the mean percentage of induced apoptotic cells was significantly ( $p < 0.05$ ) lower than that induced by PTX (Figure 3c).

Taken together, these results indicated that the PTX-OCT conjugates inhibited the growth and induced apoptosis of SSTRs-positive NSCLC cells in a SSTRs-mediated manner, whereas they were less toxic to SSTRs (2, 3, and 5)-negative cells.

### MDR-1, MRP-1, and BCRP mRNA expressions in vitro and in nude mice treated with cytotoxic conjugates or PTX

Acquired MDR is an important mechanism for PTX resistance, and herein, we addressed the effect of cytotoxic conjugates on the expressions of MDR-1, MRP-1, and BCRP in A549 cells both in vitro (Figure 4a) and in vivo (Figure 4b) by qPCR. Following 50 nmol/L PTX treatment for 96 h in vitro, the expression of MDR-1 was increased by 5.2-fold and that of MRP-1 was increased by 3.3-fold. PTX-OCT induced 1.8-fold increase of MDR-1 expression, which was significantly ( $p < 0.01$ ) lower than that induced by PTX, whereas no difference was found in MRP-1 expression. 2PTX-OCT also increased the expressions of MDR-1 (2.8-fold,  $p < 0.01$  vs. PTX) and MRP-1 (2.1-fold,  $P < 0.05$  vs. PTX), the inductive effect of which was significantly ( $p < 0.05$ ) stronger than that of PTX-OCT.

We have previously shown that 2PTX-OCT significantly inhibited tumor growth in vivo with less toxicity than PTX.<sup>16</sup> In this study, the same regimens of PTX or PTX-OCT conjugates (150 nmol/kg) were given to A549-bearing

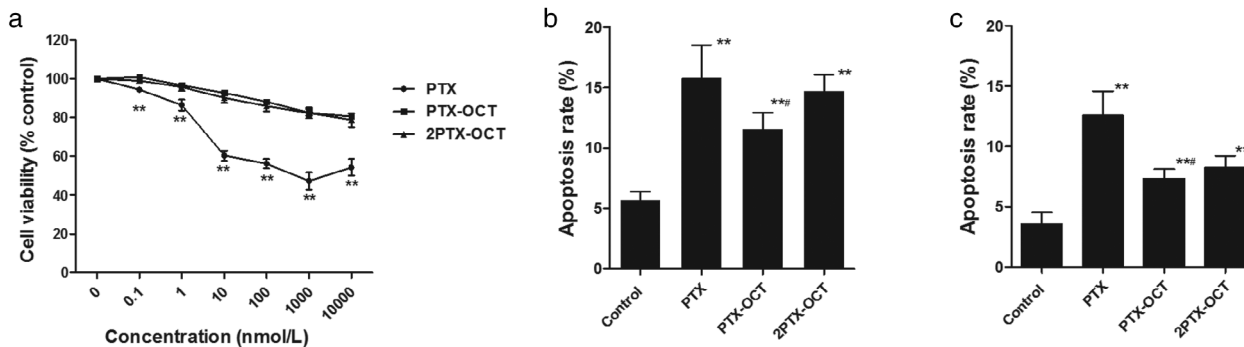


**FIGURE 3** Cytotoxicity and apoptosis induced by paclitaxel (PTX) or paclitaxel-octreotide (PTX-OCT) conjugates in H157 and A549 cells. (a) H157 cells were treated with the indicated concentration of PTX or PTX-OCT conjugates for 96 h, and cell viability was assessed by MTT assay. PTX-OCT and 2PTX-OCT showed less toxicity on H157 cells, compared with PTX, from the concentration of 0.1 nmol/L to 10  $\mu$ mol/L (\*\* $p < 0.01$ ). (b) and (c) Cell apoptosis was assessed by flow cytometry after treating A549 (b) or H157 (c) cells with 10 nmol/L PTX or PTX-OCT conjugates and staining with Annexin V and propidium iodide for 48 h. \*\* $p < 0.01$  versus control; # $p < 0.05$  versus PTX

**TABLE 1** IC<sub>50</sub> (nmol/L) of PTX, PTX-OCT, and 2PTX-OCT on growth of A549 and its paclitaxel-resistant sublines

Cell lines	PTX	PTX-OCT	2PTX-OCT
A549	65.35 ± 7.94	221.35 ± 10.60**	70.86 ± 14.12 <sup>#</sup>
A549-P	377.42 ± 38.34	305.39 ± 26.18*	206.18 ± 12.94** <sup>#</sup>
A549-PS	1457.25 ± 138.57	509.17 ± 58.66**	318.39 ± 37.35** <sup>#</sup>
A549-S	658.04 ± 47.41	128.30 ± 16.64**	111.21 ± 15.63**

Note: IC<sub>50</sub> values were mean ± SD, *n* = 3/group.

\**p* < 0.05 versus PTX group; \*\**p* < 0.01 versus PTX group. <sup>#</sup>*p* < 0.05 versus PTX-OCT group;

<sup>#</sup>*p* < 0.01 versus PTX-OCT group.

nude mice, and similar tumor growth inhibition was observed (data not shown). Interestingly, *in vivo* therapy with three administrations of PTX induced 2.7-fold upregulation of MDR-1 mRNA and 2.1-fold upregulation of MRP-1 mRNA, whereas PTX-OCT or 2PTX-OCT administration *in vivo* induced milder upregulation of MRP-1 mRNA (1.5-fold for PTX-OCT and 1.7-fold for 2PTX-OCT, *p* < 0.01 vs. PTX group), and failed to upregulate the expression of MDR-1 mRNA (*p* < 0.01 vs. PTX group). No alteration of BCRP mRNA was observed either *in vitro* or *in vivo*.

### PTX-OCT conjugates partially reversed PTX resistance in A549 PTX-resistant cells

PTX resistance is one of the main obstacles for the clinical use of PTX.<sup>22</sup> Three PTX-resistant sublines, A549-P, A549-PS, and A549-S, were derived from human A549 cells, which had different biological characteristics including morphology and doubling time (data not shown). The three PTX-resistant sublines showed different degrees of drug sensitivity toward PTX (Table 1); The RI of A549-P, A549-PS, and A549-S was 6, 22, and 10, respectively.

We next investigated the effect of PTX-OCT conjugates on the growth of PTX-resistant cells (Table 1). A549-P cells were found slightly (*p* < 0.05) more sensitive toward PTX-OCT than PTX; compared with PTX-OCT, 2PTX-OCT was more (*p* < 0.01) effective in inhibiting the growth of A549-P cells. PTX-OCT and 2PTX-OCT both showed stronger growth inhibitory effect on A549-PS cells following a similar manner of A549-P, whereas the IC<sub>50</sub> was less than that of PTX (PTX-OCT, 2.9-fold; 2PTX-OCT, 4.6-fold). A549-S cells were more sensitive toward both PTX-OCT and 2PTX-OCT, which was demonstrated by the decreased IC<sub>50</sub> by more than 5-fold and the insignificant difference in effectiveness observed between the two conjugates. These cell viability assays showed that the A549 PTX-resistant cells induced by different means were more sensitive toward cytotoxic conjugates than toward PTX.

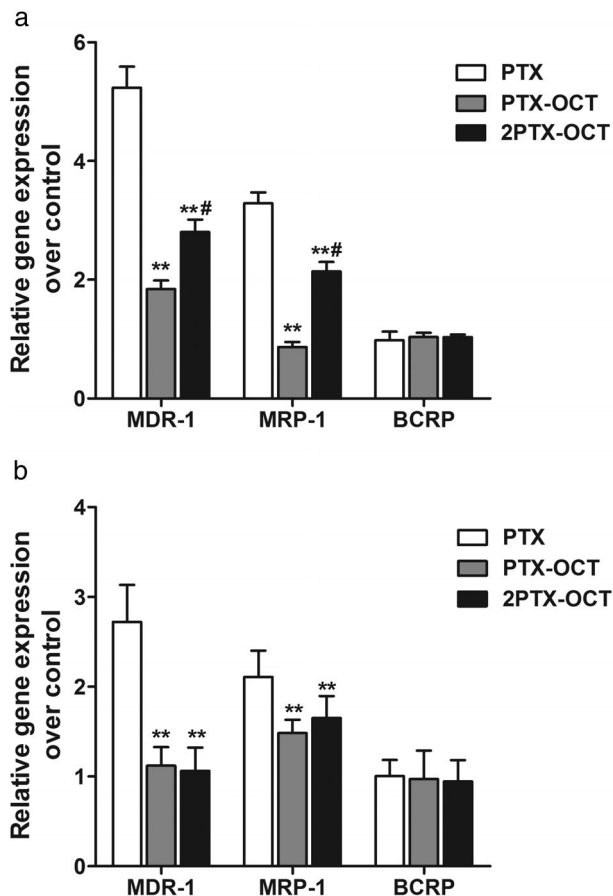


**FIGURE 4** Effect of paclitaxel-octreotide (PTX-OCT) conjugates and paclitaxel (PTX) on the expression of MDR-1, MRP-1 and BCRP mRNA *in vitro* and *in vivo*. (a) After exposure to 50 nmol/L PTX, PTX-OCT, 2PTX-OCT, or solvent control for 96 h, total RNA was extracted from the treated A549 cells and reversely transcribed, and the mRNA expressions of MDR-1, MRP-1, and BCRP were measured by qPCR with  $\beta$ -actin as the internal control. The results are expressed as fold changes of mRNA levels against control A549 cells. \*\**p* < 0.01 versus PTX; <sup>#</sup>*p* < 0.05 versus PTX-OCT. (b) Mice bearing A549 xenografts were given three intravenous injections of 150 nmol/kg of PTX, PTX-OCT, 2PTX-OCT, or solvent control on Days 1, 7, and 21. On Day 42, the mice were euthanized and tumors were excised. The mRNA expressions of MDR-1, MRP-1, and BCRP in the tumors were detected by qPCR with  $\beta$ -actin as the internal control. The results are expressed as fold changes of mRNA levels against the control group. \**p* < 0.05 versus PTX; \*\**p* < 0.01 versus PTX

### Cell-cycle distribution and the expressions of MDR-1, MRP-1, and BCRP in A549 PTX-resistant derivatives

DNA flow cytometry was performed to analyze the cell-cycle distribution of A549 PTX-resistant subtypes. Compared with the parental A549 cells, more A549-PS and A549-P cells were accumulated in G1 phase, whereas less were in S phase (*p* < 0.01) (Table 2). Interestingly, more A549-S cells were in G2/M phase, and PTX is known as a cell-cycle-specific anti-cancer agent.

Increased efflux of drugs mediated by MDR-1, MRP-1, and BCRP is a dominant mechanism for MDR of cancer cells. As shown in Figure 5, the mRNA expression of

**TABLE 2** Cell-cycle distribution of A549 and its paclitaxel-resistant sublines

	A549	A549-P	A549-PS	A549-S
G1 (%)	72.06 ± 3.14	67.12 ± 1.15*	60.94 ± 0.49**	57.39 ± 2.00**
S (%)	20.27 ± 1.80	25.18 ± 0.74*	33.31 ± 0.65**	29.91 ± 3.79*
G2/M (%)	7.68 ± 1.34	7.70 ± 0.86	5.75 ± 1.13	12.70 ± 1.80*

Note: Percentages were mean ± SD.

\* $p < 0.05$  versus A549 group; \*\* $p < 0.01$  versus A549 group.

MDR-1 was significantly increased in A549-PS cells (8.8-fold;  $p < 0.01$  compared with A549 cells) and was found the highest in A549-S cells (12.6-fold;  $p < 0.01$  compared with A549 cells;  $p < 0.01$  compared with A549-PS cells). Meanwhile, the mRNA expression of MRP-1 was significantly ( $p < 0.01$ ) higher in A549-P and A549-S cells than that in A549 cells. No significant difference in BCRP mRNA expression was found between A549 subtypes and the parental cells.

## DISCUSSION

To date, at least five different human SSTR subtypes (SSTR1-5) have been characterized that are widely expressed in various neoplastic and physiological tissues.<sup>23,24</sup> Several studies have shown that SSTRs are overexpressed in NSCLC using radio-labeled analogs.<sup>25</sup> In this study, we examined the expressions of SSTR2 and SSTR5 in NSCLC by immunohistochemistry and detected them in both cell membrane and cytoplasm. Their expressions were significantly increased in NSCLC samples (>60%) than in peri-tumor normal tissues (<20%). These findings provide the possibility of developing SSTRs-mediated targeted chemotherapy for NSCLC treatment.

Using peptides as carriers delivering cytotoxic agents to target their specific receptors on cancer cells serves as a strategy of targeted chemotherapy, aiming at solving the limitations of conventional chemotherapy, including adverse side effects, low efficacy, and drug resistance. Many cytotoxic analogs of luteinizing hormone-releasing hormone (LH-RH), somatostatin, bombesin, and other peptides have been developed, in which the peptides are linked with different chemotherapeutic agents such as doxorubicin (DOX), 2-pyrrolino-DOX, camptothecin, methotrexate, and PTX. Clinical trials using these analogs are still in progress.<sup>26-29</sup> Our group synthesized two cytotoxic somatostatin analogs, PTX-OCT and 2PTX-OCT, by coupling PTX to somatostatin analog octreotide. The two conjugates selectively inhibited the growth of NSCLC cells in vitro,<sup>15</sup> and 2PTX-OCT exerted a stronger tumor growth inhibitory effect on nude mice with reduced toxicity compared to PTX.<sup>16</sup> In the current study, we further investigated the effect of the cytotoxic conjugates on NSCLC cell apoptosis. Octreotide is an analog of somatostatin and preferably binds to SSTR2, SSTR3, and SSTR5.<sup>28</sup> H157 cells were tested as the negative

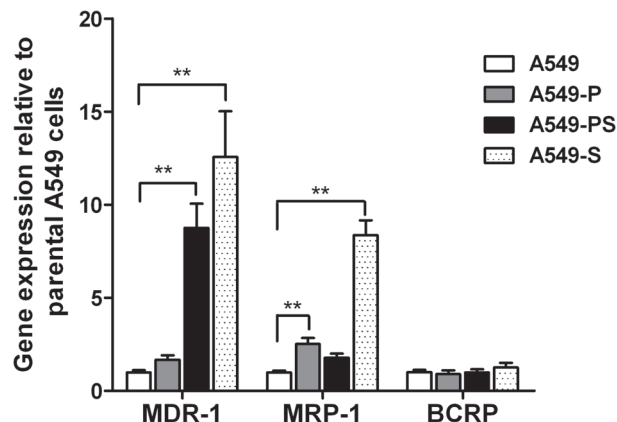


**FIGURE 5** MDR-1, MRP-1, and BCRP expressions in A549 paclitaxel (PTX)-resistant sublines. Total RNA from A549 cells and the three PTX-resistant sublines was isolated and reversely transcribed. The mRNA expressions of MDR-1, MRP-1, and BCRP were measured by qPCR with  $\beta$ -actin as the internal control. The results are expressed as fold changes of mRNA levels against the parental A549 cells (arbitrarily defined as 1). \*\* $p < 0.01$

control, and no SSTR2, SSTR3, or SSTR5 mRNA expression was detected, which was consistent with the previous report.<sup>29</sup> PTX-OCT conjugates showed a similar effect as PTX on inducing apoptosis of SSTRs-positive A549 cells. For H157 cells, apoptosis was also observed following the treatments of the conjugates, whereas the apoptotic rate was much lower than that induced by PTX at the same concentration.

In addition to the toxic side effects of PTX on normal tissues, PTX resistance, including acquired and intrinsic resistance, is another major obstacle for treating NSCLC patients. It has been demonstrated that PTX resistance could be induced by the altered tubulin expression patterns,<sup>30</sup> and could also be mediated by MDR. MDR is a phenomenon that in addition to the developed resistance toward a single drug, cells become cross-resistant to other structurally and mechanistically unrelated drugs. Overexpression of ABC transporters is an important mechanism for MDR<sup>31</sup> and these transporters include P-glycoprotein (PGP), MRP-1, and BCRP. PGP, the product of MDR-1 gene, is a major ABC transporter for drug efflux that modulates PTX resistance.<sup>19</sup> Because of the hydrophobic nature, PTX can induce MDR phenotype through overexpressing MDR-1.<sup>32</sup> In the present study, moderate induction of the mRNA expressions of MDR-1 and MRP-1 was observed following PTX-OCT treatment in vitro. 2PTX-OCT also exhibited moderate induction of MDR-1 expression in vitro, whereas no significant difference in MRP-1 induction was observed between PTX and 2PTX-OCT. Neither PTX-OCT nor 2PTX-OCT induced MDR-1 overexpression in vivo, whereas PTX or cytotoxic conjugates elevated the expression of MRP-1, although the effect of PTX-OCT or 2PTX-OCT was much lower than that of PTX. These results indicated that targeted somatostatin analogs might delay the development of acquired resistance both in vitro and in vivo.

To elucidate the potential mechanisms of PTX resistance, numerous drug-resistant sublines have been established *in vitro* or *in vivo*. *In vitro* establishment of drug-resistant sublines is usually through exposure to drugs of low concentrations in a stepwise manner, and sometimes through pulse exposure to high-dose drugs. Herein, three A549 PTX-resistant sublines were selected by different approaches, including pulse exposure (A549-P), stepwise culture (A549-S), and pulse exposure followed by stepwise culture (A549-PS). Obvious changes in the morphology and doubling time of the PTX-resistant derivatives were observed, in comparison with their parental cells (data not shown), and they also exhibited different levels of drug resistance toward PTX. As expected, the A549-PS cell line was the most resistant toward PTX, with a 22-fold higher  $IC_{50}$  than that of the A549 cell line. The cells seem to develop drug resistance more easily through stepwise culture in PTX than through pulse exposure. Meanwhile, A549-S cells were overall significantly more resistant toward PTX than A549-P cells.

Targeted chemotherapy can reduce toxicity to normal cells and might be more efficacious against drug-resistant cancer cells. Compared to PTX, the targeted conjugates PTX-OCT and 2PTX-OCT showed higher cytotoxicity on all the three PTX-resistant cells. Both A549-P and A549-PS cells were more sensitive toward 2PTX-OCT than toward PTX-OCT, whereas A549-S subline showed similar sensitivity toward the two conjugates. Moreover, A549-S cells were the most sensitive toward PTX-OCT conjugates among the three PTX-resistant sublines, as reflected by both the lowest value (5-fold decrease) of  $IC_{50}$ .

The expressions of MDR genes in the selected PTX-resistant sublines were further analyzed. Numerical increase of MDR-1 expression was observed in A549-P cells, whereas 9-fold upregulation of MDR-1 was observed in A549-PS cells. MDR-1 expression was elevated the most (~13-fold) in A549-S sublines that were selected in a stepwise manner and under low-dose PTX. Horwitz et al.<sup>33</sup> established two A549 PTX-resistant derivatives, A549-T12 and A549-T24, by means of stepwise culture in increasing low-dose Taxol, and they were 9- and 12-fold resistant toward Taxol, respectively. However, they found that PGP was not expressed in A549-T12 and only low level of PGP expression was detected in A549-T24 by qPCR, which was inconsistent with our findings. The inconsistency might be attributed to the Taxol-dependency of A549-T12 and A549-T24 normal cell growth. We identified different biological characteristics of A549-S cells, which grew independently of PTX. Such a discrepancy might be attributed to the use of different methods for MDR-1 detection. The role of MRP-1 in PTX resistance is not conclusive.<sup>34,35</sup> Overexpression of MRP-1 by different folds was detected in A549-P and A549-S cells. Interestingly, no significant change of MRP-1 expression was observed in A549-PS cells. As another member of ABC transporters, BCRP did not induce any changes of the resistant cell lines. Overall, the three PTX-resistant A549 sublines were successfully established with MDR-related gene expressions.

As mentioned above, overexpression of MDR-related genes, including MDR-1 and MRP-1, was induced in A549-S cells. Therefore, cytotoxic somatostatin analogs might be more toxic to PTX-resistant cells with MDR phenotype. Another reason for the higher sensitivity of A549-S cells toward PTX-OCT conjugates is that A549-S cells had a distinct cell-cycle distribution revealed by FACS analysis.

The mechanism through which PTX-OCT conjugates could overcome PTX resistance and reduce MDR gene expressions in A549 cells has not been clearly elucidated, which might involve several mechanisms. First, higher concentration of cytotoxic analogs was delivered to target tumor cells with internalization of PTX mediated by SSTRs. Second, internalization of PTX by SSTRs might partially evade the effect of the efflux pump system of MDR. After linking to octreotide, the conjugates becomes more hydrophilic, whereas PTX itself is a hydrophobic compound. Hydrophilic drugs are more soluble in water and can readily permeate into tissues. Therefore, the cytotoxic conjugates are more easily delivered into target tumor tissues and have less effect on inducing MDR genes. This might also explain the observed precipitation of PTX at higher concentrations (such as 10  $\mu\text{mol/L}$ ), no stronger inhibitory effect was detected by increasing the drug concentration, whereas PTX-OCT conjugates were more cytotoxic than PTX at higher concentrations.<sup>15</sup>

In conclusion, this study further demonstrated that PTX-OCT conjugates could significantly inhibit the growth and induce apoptosis of NSCLC cells, which was at least partially mediated by SSTRs. Meanwhile, PTX linking to somatostatin analog showed enhanced efficacy on PTX-resistant sublines that were established through different approaches. In addition, no or mild induction of MDR-1, MRP-1, and BCRP gene expressions was observed both *in vitro* and *in vivo* following treatment with cytotoxic conjugates as compared to PTX treatment. Our findings suggest that PTX-OCT conjugates could be a promising treatment for NSCLC, especially for that with PTX resistance and with delayed MDR development.

## ACKNOWLEDGMENTS

This work was supported by the Shandong Provincial Natural Science Foundation (ZR2020MH236), the National Natural Science Foundation of China (81874044), and the Beijing Xisike Clinical Oncology Research Foundation (Y-QL2019-0376).

## CONFLICT OF INTEREST

The authors declared that they have no conflict of interest to this work.

## ORCID

Xiuwen Wang  <https://orcid.org/0000-0001-6494-122X>

## REFERENCES

1. Sung H, Ferlay J, Siegel RL, Laversanne M, Soerjomataram I, Jemal A, et al. Global cancer statistics 2020: GLOBOCAN estimates of

- incidence and mortality worldwide for 36 cancers in 185 countries. *CA Cancer J Clin.* 2021;71:209–49. <https://doi.org/10.3322/caac.21660>
2. Wei W, Zeng H, Zheng R, Zhang S, An L, Chen R, et al. Cancer registration in China and its role in cancer prevention and control. *Lancet Oncol.* 2020;21:e342–9. [https://doi.org/10.1016/S1470-2045\(20\)30073-5](https://doi.org/10.1016/S1470-2045(20)30073-5)
  3. Thai AA, Solomon BJ, Sequist LV, Gainor JF, Heist RS. Lung cancer. *Lancet.* 2021;398:535–54. [https://doi.org/10.1016/S0140-6736\(21\)00312-3](https://doi.org/10.1016/S0140-6736(21)00312-3)
  4. Vasan N, Baselga J, Hyman DM. A view on drug resistance in cancer. *Nature.* 2019;575:299–309. <https://doi.org/10.1038/s41586-019-1730-1>
  5. Yang CH, Horwitz SB. Taxol([R]): the first microtubule stabilizing agent. *Int J Mol Sci.* 2017;18:1733. <https://doi.org/10.3390/ijms18081733>
  6. Bedard PL, Hyman DM, Davids MS, Siu LL. Small molecules, big impact: 20 years of targeted therapy in oncology. *Lancet.* 2020;395:1078–88. [https://doi.org/10.1016/S0140-6736\(20\)30164-1](https://doi.org/10.1016/S0140-6736(20)30164-1)
  7. Zheng K, Chen R, Sun Y, Tan Z, Liu Y, Cheng X, et al. Cantharidin-loaded functional mesoporous titanium peroxide nanoparticles for non-small cell lung cancer targeted chemotherapy combined with high effective photodynamic therapy. *Thorac Cancer.* 2020;11:1476–86. <https://doi.org/10.1111/1759-7714.13414>
  8. Chatzisdieri T, Leonidis G, Sarli V. Cancer-targeted delivery systems based on peptides. *Future Med Chem.* 2018;10:2201–26. <https://doi.org/10.4155/fmc-2018-0174>
  9. Herlin G, Kölbeck KG, Menzel PL, Svensson L, Aspelin P, Capitanio A, et al. Quantitative assessment of <sup>99m</sup>Tc-depreotide uptake in patients with non-small-cell lung cancer: immunohistochemical correlations. *Acta Radiol.* 2009;50:902–8.
  10. Eychenne R, Bouvry C, Bourgeois M, Loyer P, Benoist E, Lepareur N. Overview of radiolabeled somatostatin analogs for cancer imaging and therapy. *Molecules.* 2020;25:4012. <https://doi.org/10.3390/molecules25174012>
  11. Liu F, Guo X, Liu T, Xu X, Li N, Xiong C, et al. Evaluation of pan-SSTRs targeted Radioligand [(64)cu]NOTA-PA1 using micro-PET imaging in Xenografted mice. *ACS Med Chem Lett.* 2020;11:445–50. <https://doi.org/10.1021/acsmchemlett.9b00544>
  12. Hohla F, Buchholz S, Schally AV, Krishan A, Rick FG, Szalontay L, et al. Targeted cytotoxic somatostatin analog AN-162 inhibits growth of human colon carcinomas and increases sensitivity of doxorubicin resistant murine leukemia cells. *Cancer Lett.* 2010;294:35–42. <https://doi.org/10.1016/j.canlet.2010.01.018>
  13. Seitz S, Buchholz S, Schally AV, Jayakumar AR, Weber F, Papadia A, et al. Targeting triple-negative breast cancer through the somatostatin receptor with the new cytotoxic somatostatin analogue AN-162 [AEZS-124]. *Anticancer Drugs.* 2013;24:150–7. <https://doi.org/10.1097/CAD.0b013e32835a7e29>
  14. Pozsgai E, Schally AV, Halmos G, Rick F, Bellyei S. The inhibitory effect of a novel cytotoxic somatostatin analogue AN-162 on experimental glioblastoma. *Horm Metab Res.* 2010;42:781–6. <https://doi.org/10.1055/s-0030-1261955>
  15. Sun ML, Wei JM, Wang XM, Li L, Wang P, Li M, et al. Paclitaxel-octreotide conjugates inhibit growth of human non-small cell lung cancer cells in vitro. *Exp Oncol.* 2007;29:186–91.
  16. Shen H, Hu D, Du J, Wang X, Liu Y, Wang Y, et al. Paclitaxel-octreotide conjugates in tumor growth inhibition of A549 human non-small cell lung cancer xenografted into nude mice. *Eur J Pharmacol.* 2008;601:23–9.
  17. Yusuf RZ, Duan Z, Lamendola DE, Penson RT, Seiden MV. Paclitaxel resistance: molecular mechanisms and pharmacologic manipulation. *Curr Cancer Drug Targets.* 2003;3:1–19. <https://doi.org/10.2174/1568009033333754>
  18. Gottesman MM, Hrycyna CA, Schoenlein PV, Germann UA, Pastan I. Genetic analysis of the multidrug transporter. *Annu Rev Genet.* 1995;29:607–49.
  19. Xiao H, Zheng Y, Ma L, Tian L, Sun Q. Clinically-relevant ABC transporter for anti-cancer drug resistance. *Front Pharmacol.* 2021;12:648407. <https://doi.org/10.3389/fphar.2021.648407>
  20. Buchholz S, Keller G, Schally AV, Halmos G, Hohla F, Heinrich E, et al. Therapy of ovarian cancers with targeted cytotoxic analogs of bombesin, somatostatin, and luteinizing hormone-releasing hormone and their combinations. *Proc Natl Acad Sci U S A.* 2006;103:10403–7.
  21. Verma K, Ramanathan K. Investigation of paclitaxel resistant R306C mutation in beta-tubulin-a computational approach. *J Cell Biochem.* 2015;116:1318–24. <https://doi.org/10.1002/jcb.25087>
  22. Xiao H, Verdier-Pinard P, Fernandez-Fuentes N, Burd B, Angeletti R, Fiser A, et al. Insights into the mechanism of microtubule stabilization by Taxol. *Proc Natl Acad Sci U S A.* 2006;103:10166–73. <https://doi.org/10.1073/pnas.0603704103>
  23. Hofland LJ, Lamberts SW. Somatostatin receptor subtype expression in human tumors. *Ann Oncol.* 2001;12(suppl 2):S31–6.
  24. Hofsl E. The somatostatin receptor family—a window against new diagnosis and therapy of cancer. *Tidsskr Nor Laegeforen.* 2002;122:487–91.
  25. Sun L, Coy DH. Somatostatin and its analogs. *Curr Drug Targets.* 2016;17:529–37. <https://doi.org/10.2174/1389450116666141205163548>
  26. Seitz S, Buchholz S, Schally AV, Weber F, Klinkhammer-Schalke M, Inwald EC, et al. Triple negative breast cancers express receptors for LHRH and are potential therapeutic targets for cytotoxic LHRH-analogs, AEZS 108 and AEZS 125. *BMC Cancer.* 2014;14:847. <https://doi.org/10.1186/1471-2407-14-847>
  27. Steven SY, Athreya K, Liu SV, Schally AV, Tsao-Wei D, Groshen S, et al. A phase II trial of AEZS-108 in castration- and Taxane-resistant prostate cancer. *Clin Genitourin Cancer.* 2017;15:742–9. <https://doi.org/10.1016/j.clgc.2017.06.002>
  28. Lamberts SW, van der Lely AJ, de Herder WW, Hofland LJ. Octreotide. *N Engl J Med.* 1996;334:246–54.
  29. Kiaris H, Schally AV, Nagy A, Szepesházi K, Hebert F, Halmos G. A targeted cytotoxic somatostatin (SST) analogue, AN-238, inhibits the growth of H-69 small-cell lung carcinoma (SCLC) and H-157 non-SCLC in nude mice. *Eur J Cancer.* 2001;37:620–8.
  30. Jin J, Pastrello D, Penning NA, Jones AT. Clustering of endocytic organelles in parental and drug-resistant myeloid leukaemia cell lines lacking centrosomally organised microtubule arrays. *Int J Biochem Cell Biol.* 2008;40:2240–52. <https://doi.org/10.1016/j.biocel.2008.03.004>
  31. Choi YH, Yu AM. ABC transporters in multidrug resistance and pharmacokinetics, and strategies for drug development. *Curr Pharm Des.* 2014;20:793–807. <https://doi.org/10.2174/138161282005140214165212>
  32. He Y, Liang S, Long M, Xu H. Mesoporous silica nanoparticles as potential carriers for enhanced drug solubility of paclitaxel. *Korean J Couns Psychother.* 2017;78:12–7. <https://doi.org/10.1016/j.msec.2017.04.049>
  33. Kavallaris M, Kuo DY, Burkhart CA, Regl DL, Norris MD, Haber M, et al. Taxol-resistant epithelial ovarian tumors are associated with altered expression of specific beta-tubulin isotypes. *J Clin Invest.* 1997;100:1282–93.
  34. He SM, Li R, Kanwar JR, Zhou SF. Structural and functional properties of human multidrug resistance protein 1 (MRP1/ABCC1). *Curr Med Chem.* 2011;18:439–81. <https://doi.org/10.2174/092986711794839197>
  35. Cole SP. Multidrug resistance protein 1 (MRP1, ABCC1), a “multi-tasking” ATP-binding cassette (ABC) transporter. *J Biol Chem.* 2014;289:30880–8. <https://doi.org/10.1074/jbc.R114.609248>

**How to cite this article:** Liu Y, Xia H, Wang Y, Han W, Qin J, Gao W, et al. Targeted paclitaxel-octreotide conjugates inhibited the growth of paclitaxel-resistant human non-small cell lung cancer A549 cells in vitro. *Thorac Cancer.* 2021;12:3053–61. <https://doi.org/10.1111/1759-7714.14182>